J Surfact Deterg (2020)
DOI 10.1002/jsde.12473

ORIGINAL ARTICLE

New Biodegradable Nonionic-Anionic Surfactants Based on Different Fatty Alcohols as Corrosion Inhibitors for Aluminum in Acidic Medium

Manal El Hefnawy[1] · **Mohamed Deef Allah**[1] · **Samar Abd Elhamed**[1]

Received: 9 July 2020 / Revised: 1 October 2020 / Accepted: 26 October 2020

Abstract Two series of eco-friendly nonionic anionic surfactants based on itaconic acid and 1, 6 hexane diol were synthesized. The chemical structures of the prepared surfactant were confirmed by FTIR and ^{1}H NMR spectroscopy. The prepared surfactants were evaluated to prevent the corrosion of aluminum in 1.0 M HCl solution by electrochemical and chemical methods. The data obtained showed that the prepared compounds have good inhibition efficiency (IE%) even at 10^{-5} M concentrations and act as mixed-type inhibitors, they do not affect the mechanism of the electrode processes, as well as the IE% increase by increasing the concentrations of the inhibitors, immersion time, and hydrophilic chain length. The high inhibition efficiency is due to the adsorption of the inhibitors molecules on the metal surface and the formation of a protective film. The surface activities of these compounds were also investigated and were correlated to their inhibition efficiencies and chemical structure. Through studying biodegradability of the synthesized surfactants we find that they are readily biodegradable in the environment and thus they are considered as eco-friendly corrosion inhibitors. Finally, the effect of the addition of these compounds on the aluminum surface was identified by atomic force microscopy (AFM) technique.

Keywords Nonionic-anionic · Eco-friendly · Inhibitors · Aluminum · AFM

J Surfact Deterg (2020).

Supporting information Additional supporting information may be found online in the Supporting Information section at the end of the article.

✉ Manal El Hefnawy
manalelhefnawy@yahoo.com

[1] Basic Science Department, Faculty of Engineering, Benha University, 108 Shoubra street, Shoubra, 11629, Egypt

Introduction

The most attractive element in many industrial applications is aluminum; which is included in automotive, marine, and aerospace, pharmaceutical products, packaging for food and beverages (Abdallah et al., 2015; Bardal, 2004; Winston and Uhlig, 2011) due to its high thermal and electrical conductivity, excellent formability, light weight, and low cost. In addition to its good corrosion resistance in the atmosphere and among aqueous medium (Kaufman, 2000;Yuan-Ting et al., 2017) since it forms a resistive oxide layer on its surface protects it from corrosion but this layers in chloride containing solution, alkaline, and acidic medium destroyed. Several methods have been used to stifle the corrosion of aluminum in acidic media, the most applicable method is the use of organic compounds (Abdallah et al., 2018b; Li et al., 2011, 2014; Safek et al., 2012; Solmaz et al., 2008; Zapta-Loria and Pech-Canul, 2014); as they form an adsorbing layer on the metal surface protecting it from the corrosive solutions (Abdallah et al., 2018a; Al-Khaldi and Al-Qahtani, 2013; Lece et al., 2008).However, most of these compounds have damaging effects on human health and the atmosphere. One of the most important classes of organic compounds are surfactants; which are used as corrosion inhibitors due to their lower toxicity, simple and economical production in addition to their higher capability to absorb at the metal surface forming a layer that protects metals from corrosive medium (Mehdaoui et al., 2015; Migahed et al., 2016; Saban et al., 2015; Zhang

et al., 2011).The hydrophobic tail in the surfactant governs its migration from the solution to the solid–liquid interface and acts as a barrier film that isolates the surface of the metal from the corrosive medium; moreover, the head groups of the surfactant always contain functional groups that are rich with the electron, where those groups block the active centers of the metal surface (Fouda et al., 2019; Singh and Quraish, 2011). Scientists have attempted to produce new compounds to achieve more economic, ecofriendly, and efficient inhibitor. Anionic-nonionic surfactants are alkyl polyethoxylate compounds which have an anionic head at the end of the molecule (Liu et al., 2014; Wang et al., 2007). Their unique molecular structure allows them to have the properties of both anionic and nonionic surfactants, which improve surface properties (Zaho and Zhu, 2003). It also contains cleavable groups; like esters, amide, and ethoxylate groups between hydrophilic and hydrophobic groups, which make it easily hydrolyzed into the primary components (Hellberg, 2003; Lif, 1998; Negm et al., 2015, 2016; Stjerndahl et al., 2003a, b; Stjerndahl and Holmberg, 2005).

The replacement of toxic and non-biodegradable surfactants from commercial use with green and biodegradable one is highly required, in this paper, we prepared two novel series of eco-friendly nonionic-anionic surfactants based on fatty alcohols and the efficiency of these surfactants to inhibit corrosion for aluminum in acidic medium was studied by several chemical and electrochemical methods. Furthermore, the surface activity, surface morphology, and biodegradability of the synthesized surfactants were evaluated and correlated to their inhibition efficiency.

Experimental Techniques

Materials

Octanol (99%) and cetyl alcohol (99%), p-toluene sulfonic acid (99%), sodium bisulfite (95%), and propylene oxide (98%) were used as received from Sigma–Aldrich (Germany). Itaconic acid (96%) was used as purchased from Across Organics (USA). 1, 6-hexanediol was purchased from Fisher Scientific. All solvents (xylene and petroleum ether) were dried and supplied by (Al-Gomhuria Trade Pharmaceuticals and Chemical Company, Cairo, Egypt).The aluminum rods and sheets used in the current manuscript having high purity reached 99.99% provided from the aluminum factory of Nagh Hammad in Nagh Hammad Egypt.

Synthesis of Nonionic-Anionic Surfactant

The nonionic-anionic surfactants synthesis process was carried out through four main steps as explained in Scheme 1.

Synthesis of 2-Methylidene-4-(Octyloxy)-4-Oxobutanoic Acid and 4-(Hexadecyloxy)-2-Methylidene-4-Oxobutanoic Acid

About 0.1 mol of itaconic acid reacted with octanol (0.05 mol) and with cetyl alcohol (0.05 mol) separately in 100 mL xylene as a solvent and (0.1% by weight) p-toluene sulfonic acid as a dehydrating agent with continuous water removal from the reaction in a mechanical stirrer equipped 500 mL round flask (Bedair et al., 2017; John and Haq, 1977) and a Dean-Stark connection. The distillation of xylene was carried out under reduced pressure of 20 mbar (heating bath 50°C) by rotary evaporator. The obtained compound has been washed with petroleum ether twice to ensure the removal of the unreacted fatty alcohol and dried under vacuum to eliminate the petroleum ether.

Synthesis of 1-(6-Hydroxyhexyl) 4-Octyl 2-Methylidenebutanedioate &4-Hexadecyl 1-(6-Hydroxyhexyl) 2-Methylidenebutanedioate

About 0.1 mol of the synthesized monoester compound is reacted with 0.1 mol of 1,6 hexanediol with the use of 100 mL of xylene as a solvent and 0.1% p-toluene sulphonic acid to catalyze the reaction at a temperature of 110 °C for 4 h to produce the desired diester compound (Bedair et al., 2017)

Synthesis of Nonionic Surfactants

Nonionic surfactants were synthesized by adding propylene oxide to 1-(6-hydroxyhexyl)4-octyl 2-methylidene butanedioate and to 4-hexadecyl 1-(6-hydroxyhexyl) 2-methylidenebutanedioate, respectively. The addition of propylene oxide was carried out in a dropwise manner under heating, continuous stirring, and efficient reflux with the use of KOH as a catalyst (Tantawy et al., 2014). The mass change in the reaction mixture was used to measure the reacted amount of propylene oxide and the average propoxylation degree. The reaction was carried out at different time intervals ranging from 1–10 h. The based catalyst was neutralized by adding HCl to a pH 7.(yield: Ia-c = 87% &IIa-c = 85%).

Synthesis of Nonionic-Anionic Surfactant

Sulfonation of the Products

Propoxylated1-(6-hydroxyhexyl) 4-octyl 2-methylidene butanedioate (0.1 mol)and Propoxylated4-hexadecyl 1-(6-hydroxyhexyl) 2-methylidene butanedioate prepared in the third step in ethanol each refluxed for 10–12 h with 150 mL saturated solution of sodium bisulphate and 5 g of

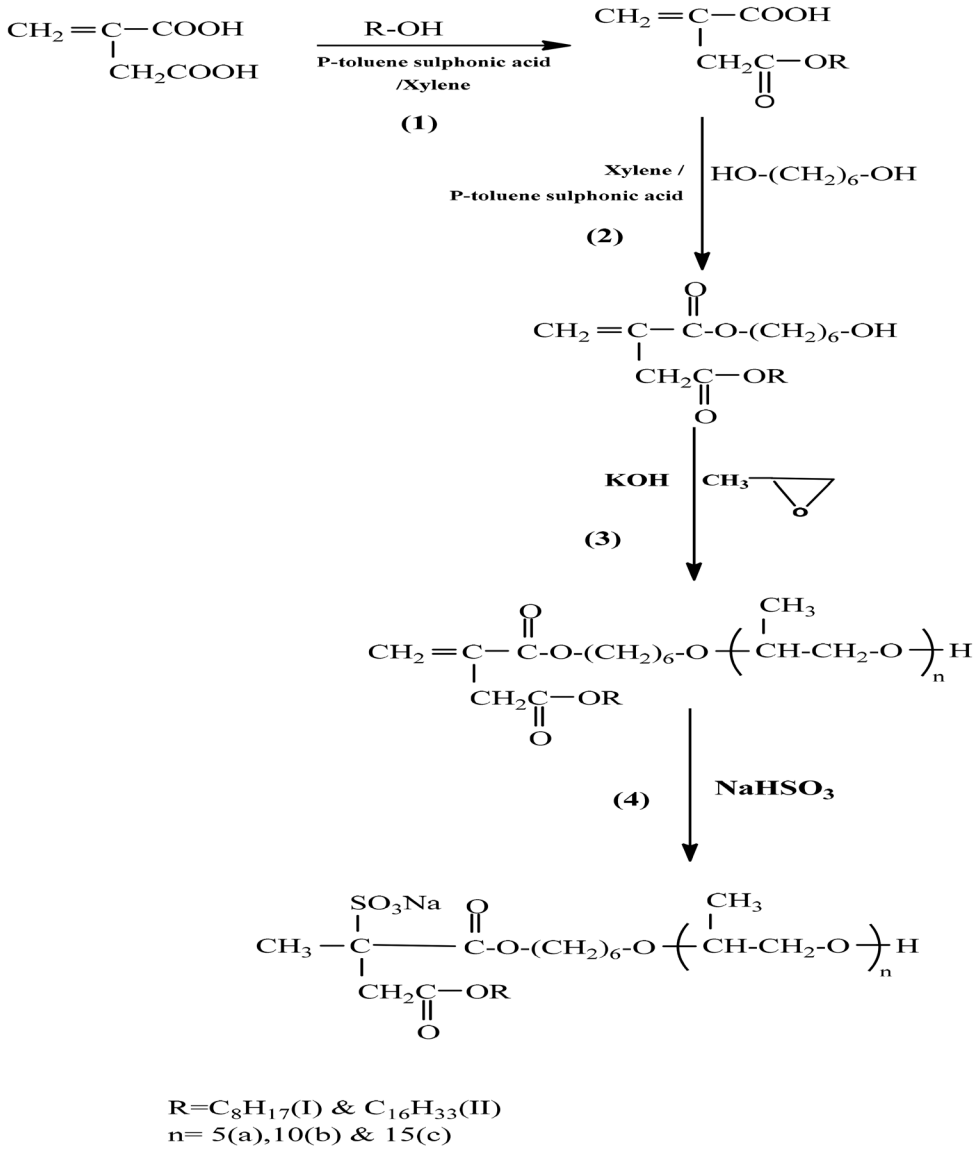

Scheme 1 Synthesis of the prepared nonionic-anionic surfactants

sodium sulfonate and, neutralized with sodium hydroxide solution to afford the required compounds, Scheme 1.

Weight Loss Method

Weight loss test was carried out three times on aluminum samples coupons with surface area 1.0 cm^2 and the weight was the average of the three coupons. The samples were mechanically polished with emery paper, ultrasonically degreased in alkaline mixtures, then after washing by distilled water use filter paper to dry them and weigh them (Tewfik and Negm, 2016).The weight loss (g/cm^2) was measured at different immersion times at a temperature of 30 °C by calculating the weight of the samples before and after immersion into 100 mL of the test solution (1.0 M HCl with and without the inhibitors).The weight loss, the corrosion rate K and the percentage inhibition efficiency % IE was determined by using the following equations (Chen et al., 2011).

$$\Delta W = W_1 - W_2 \quad (1)$$

$$K = \Delta W / St \quad (2)$$

$$\%IE = (\Delta W - \Delta W_i / \Delta W) \times 100 \quad (3)$$

W_1 and W_2 are the weights of the specimen before and after immersion into the corrosive solution, respectively, ΔW_i and ΔW are the weight losses of aluminum per unit area with and without adding the inhibitor, S is the total

surface area of the corroded sample and t is the immersion time in hours.

Electrochemical Polarization

A three-electrode cell, with platinum counter electrode and saturated calomel electrode as a reference electrode (SCE), were all used to carry out the electrochemical experiments. Aluminum working electrode was a rod impeded in a glass tube with Araldite leaving an exposed bottom side with an area of 0.1 cm^2 exposed to the corrosive solution. Different grades of emery papers were used to abrade the exposed surface then washed with both distilled water and acetone and dried using filter papers, before immersing it. The electrode was lifted in the test solution until it reaches a steady-state potential value before starting the measurements. Corrosion parameters were measured using Metrohmpotentiostat supported with Nova software for calculations. The potentiodynamic polarization measurements were obtained using a scan rate of 2 mVs^{-1} at 25 ± 1 °C. The inhibition efficiency IE attained from electrochemical polarization was determined using the following equation (Hegazy et al., 2011).

$$IE\% = \left(\frac{I_f - In}{I_f}\right) \times 100 \quad (4)$$

where I_f and I_n are the corrosion current densities without and with adding the inhibitors.

Electrochemical Impedance

Electrochemical Impedance (EIS) spectra were evaluated at open circuit potential (OCP) after immersing the electrode for 30 min. The AC signal was 5 mV peak to peak and the frequency range was between 50 kHz and 0.1 Hz by using the same Potentiostat/Galvanostat as in polarization with EIS 300 calculation software, the inhibition efficiency was obtained using Eq. (5) (Azzam and Abd El-Aal, 2013).

$$IE\% = \left[\frac{R_{cti} - R_{ctf}}{R_{cti}}\right] \times 100 \quad (5)$$

where, Rcti and R_{ctf} are the charge transfer resistances with and without adding the inhibitor.

Surface Tension and Critical Micelle Concentration

Surface tension measurements were performed by a Du -Nouy tension meter using the platinum ring detachment method (±0.5 mN/m). At 25°C, different concentration of freshly prepared aqueous solutions of the synthesized surfactants were poured into a clean Teflon cup and left for 2 min to permit complete adsorption at the solution surface and stabilization then the values of the surface tension were calculated using an average of three times, at the end, the platinum ring was washed with dilute hydrochloric acid and distilled water (Chavda et al., 2011). The CMC values were obtained through a conventional plot of surface tension *versus* the logarithm of the concentration of the surfactants.

Biodegradability

The Dü-Nouy tensiometer (Krüss type K6) was used in the determination of the biodegradability of the nonionic-anionic surfactants in river water (Tawfik, 2015). This method was carried out by incubation of 100 ppm solution of each surfactant in river water at a temperature of 30 °C, then withdrawing and filtering a sample on a daily basis (for 28 days), to measure the surface tension value. The biodegradation percent (D %) was obtained using Eq. (6).

$$D\% = (\gamma_t - \gamma_0)/(\gamma_{bt} - \gamma_0) \times 100 \quad (6)$$

where γ_t, γ_0, andγ_{bt} are the surface tension at time t, at zero time, and of the river water, respectively.

Surface Morphology

Atomic force microscopy (AFM; Pico SPM-Pico scan 2100, Molecular Imaging, Arizona, AZ, USA) was used to study the aluminum surface morphology, aluminum coupons were analyzed after 5 h of exposure time to 1.0 M HCl solutions in the absence and presence of 10^{-3} M of compound I_b and II_b.

Results and Discussion

Structure

FTIR spectra and ^{1}H-NMR Spectra were used to confirm the chemical structures of the prepared compounds in Scheme 1.

FTIR spectra of 2-methylidene-4-(octyloxy)-4-oxobutanoic acid indicate absorption bands at 3280 cm^{-1} (OH of carboxylic acid), 2850 cm^{-1} (C–H aliphatic), 1732 cm^{-1}(C=O of ester), 1710 cm^{-1} (C=O of acid), and 1628 cm^{-1} (C=C) are the most important characteristic bands (see Fig. S1).

FTIR spectra of 1-(6-hydroxyhexyl) 4-octyl 2-methylidenebutanedioate showed absorption bands at 3300 cm^{-1} (OH) group, 2840 cm^{-1} (C–H aliphatic), 1732 cm^{-1}(C=O of ester), 1710 cm^{-1} (C=O of acid), and 1630 cm^{-1} (C=C) are the most important characteristic bands (see Fig. S2).

FTIR spectra of nonionic surfactant based on octanol showed absorption bands at 3313 cm^{-1} (OH) group, 2922,

2840 cm^{-1}(C–H aliphatic), 1737 cm^{-1} (C=O of ester), 1633 cm^{-1} (C=C), and 1088 cm^{-1} (C–O–C) ether group (see Fig. S3).

FTIR spectra of nonionic-anionic surfactant compound (I_a) illustrated absorption bands at 3322 cm^{-1}(OH) group, 2940 cm^{-1} (C–H aliphatic), 1728 cm^{-1} (C=O of ester), 1430 cm^{-1} (C–O), 1160 cm^{-1} (SO_3 sulfonate group), and 1075 cm^{-1} (C–O–C) ether group (see Fig. S4).

FTIR of nonionic- anionic surfactant compound (I_b) illustrated absorption bands at 3400 cm^{-1}(OH) group, 2922–2853 cm^{-1} (C–H aliphatic), 1735 cm^{-1} (C=O of ester), 1460 cm^{-1} (C–O), 1167, 1046 cm^{-1} (SO_3 Sulfonate group), and 1088 cm^{-1} (C–O–C) ether group (Fig. 1).

FTIR of nonionic-anionic surfactant compound (I_c) illustrated absorption bands at 3320 cm^{-1} (OH) group, 2910–2860 cm^{-1} (C–H aliphatic), 1738 cm^{-1} (C=O of ester), 1150, 1030 cm^{-1} (SO_3 sulfonate group), and1090 cm^{-1} (C–O–C) ether group.

FTIR of nonionic- anionic surfactant compound (II_a) illustrated absorption bands at 3250 cm^{-1}(OH) group, 2928 cm^{-1} (C–H aliphatic), 1725 cm^{-1} (C=O of ester), 1450 cm^{-1} (C–O), 1145, 1050 cm^{-1} (SO_3 sulfonate group), and 1080 cm^{-1} (C-O-C) ether group (see Fig. S4).

FTIR of nonionic- anionic surfactant compound (II_b) illustrated absorption bands at 3330 cm^{-1} (OH) group, 2865 cm^{-1} (C–H aliphatic), 1730 cm^{-1} (C=O of ester), 1448 cm^{-1} (C–O), 1050 cm^{-1} (SO_3 sulfonate group), and 1085 cm^{-1} (C–O–C) ether group.

FTIR spectra of compound nonionic-anionic surfactant compound (II_c) illustrated absorption bands at 3436 cm^{-1} (OH) group, 2925–2856 cm^{-1} (C–H aliphatic), 1739 cm^{-1} (C=O of ester), 1460 cm^{-1} (C–O), 1175 cm^{-1} (SO_3 sulfonate group), and 1089 cm^{-1} (C–O–C) ether group Fig. 2.

^{1}H NMR Spectra

The synthesized nonionic-anionic surfactants (I_a) ^{1}H NMR (DMSO-d_6) spectrum showed different peaks at δ = 0.782 ppm (t, 3H of term **CH_3**); δ = 1.126 ppm (m, 14H) of CH_3–**$(CH_2)_7$**–)δ = 1.298–1.521 ppm (m, 12H of **$(CH_2)_6$**); δ = 2.641 ppm (t, 2H) of CH_3–$(CH_2)_7$–**CH_2**–COO); δ=3.498–3.9 ppm (m, 10H of repeated propylene oxide units); and δ = 4.670 ppm (broad S,H of **OH**).

The synthesized nonionic-anionic surfactants (I_b) ^{1}H NMR (DMSO-d_6) spectrum showed different peaks at δ = 0.835 ppm (t, 3H of term.**CH_3**); δ=1.217 ppm (m, 14H) of CH_3–**$(CH_2)_7$**–) δ = 1.383–1.433 ppm (m, 12H of **$(CH_2)_6$**); δ=2.49 ppm (t, 2H) of CH_3–$(CH_2)_7$–**CH_2**–COO);δ=3.637–3.941 ppm (m, 30H of repeated propylene oxide units); and δ=4.508 ppm (broad S,H of **OH**) (Fig. 3).

The synthesized nonionic-anionic surfactants (I_c) ^{1}H NMR (DMSO-d_6) spectrum showed different peaks at δ=0.901 ppm (t, 3H of term.**CH_3**); δ=1.314 ppm (m, 14H) of CH_3–**$(CH_2)_7$**–) δ=1.6–1.805 ppm (m, 12H of **$(CH_2)_6$**); δ=2.53 ppm (t, 2H) of CH_3–$(CH_2)_7$–**CH_2**–COO); δ=3.075–3.647 ppm (m, 30H of repeated propylene oxide units); and δ=4.821 ppm (broad S,H of **OH**). (See Fig. S5).

The synthesized nonionic-anionic surfactants (II_c) ^{1}H NMR (DMSO-d_6) spectrum showed different peaks at δ = 0.763 ppm (t, 3H of term.**CH_3**); δ=1.183 ppm (m, 30H) of CH_3–

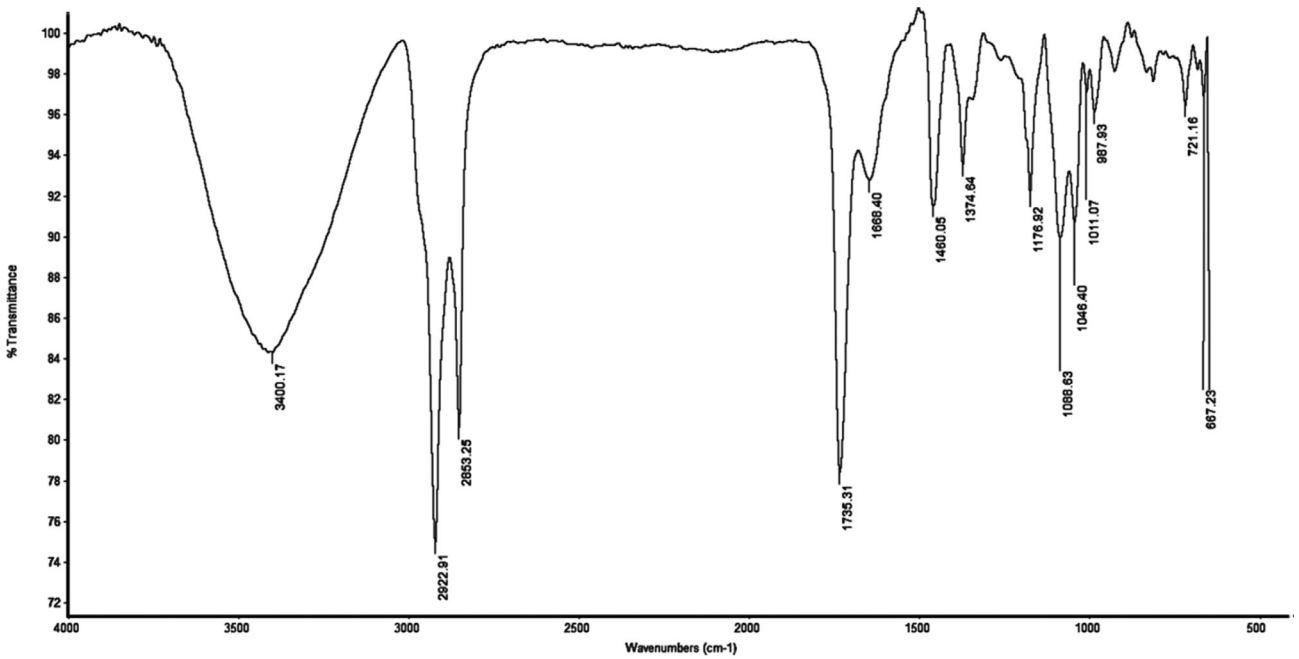

Fig 1 FTIR spectra of surfactant I_b

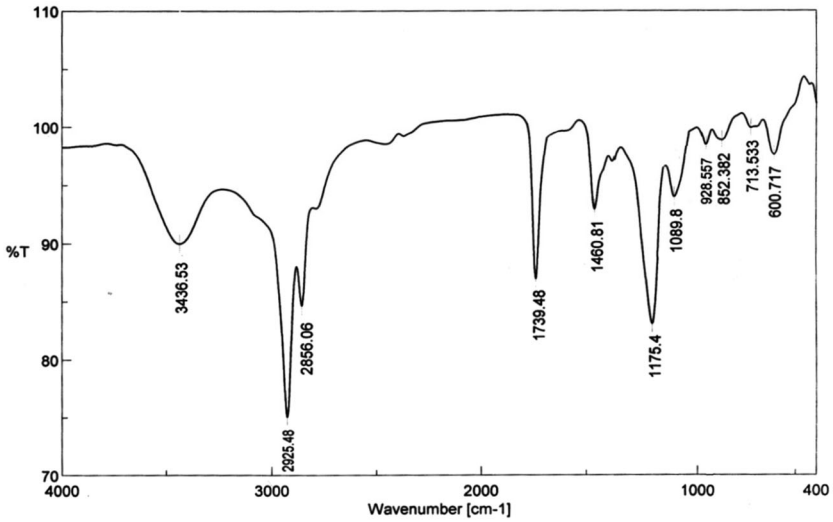

Fig 2 FTIR spectra of surfactant II_C

$(CH_2)_{15}$–) δ = 1.464 ppm (m, 12H of **$(CH_2)_6$**); δ=2.171 ppm (t, 2H) of CH_3–$(CH_2)_{15}$**–CH_2–**COO); δ = 3.401–3.485 ppm (m, 90H of the repeated propylene oxide units); and δ = 4.5824 ppm (broad S,H of **OH**) (Fig. 4).

Measurements of Weight Loss

Immersion Time Effect on Aluminum Corrosion

The weight loss was measured by using 1.0 MHCl solution in the presence and absence of the synthesized inhibitors at a constant concentration for different immersion time 60–300 min at 30 °C. The inhibition efficiencies obtained using Eq. (3) was plotted against immersion time as seen in Fig. 5.It is shown in the figure that as the immersion time increases, the IE% of different inhibitors increases gradually, the longer the immersion time the higher the IE% which attributes to the protective layer formed on the surface of aluminum, which is time-dependent (it has been stated that after a longer immersion time stable two dimensional layers from the molecules of inhibitors are formed on the metal surface (Granese et al., 1992; Rosen, 1976).

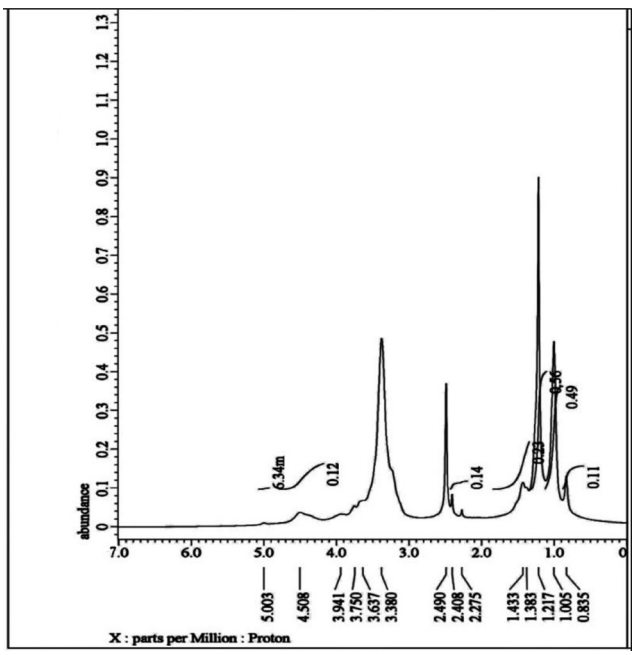

Fig 3 ^{1}H NMR spectra of surfactant I_b

Effect of Inhibitors Concentration on Aluminum Corrosion

The %IE values and rate of corrosion obtained from weight loss measurement using Eq. (3) at different concentration of the inhibitors are listed in Table 1.It is cleared that by increasing the concentration of the inhibitors the rate of corrosion decreases and the %IE increases due to the adsorption of the inhibitors at the interface of aluminum/acid solution; hence, decreasing the interactions of the corrosive ions with the metal surface. By comparing the values of IE% in Table 1, it is clear that the lower the no. of propylene oxide units in the inhibitors the lower the values of the inhibition efficiency which is a logical effect as electrons density on the inhibitors molecules increases by increasing the no of oxygen heteroatom consequently the tendency of the surfactant to be adsorbed on the aluminum surface increase (Negm et al., 2011; Xli and Mu, 2005).

Electrochemical Polarization Studies

The potentiodynamic polarization curves of aluminum in 1.0 M HCl free and inhibited with different concentration

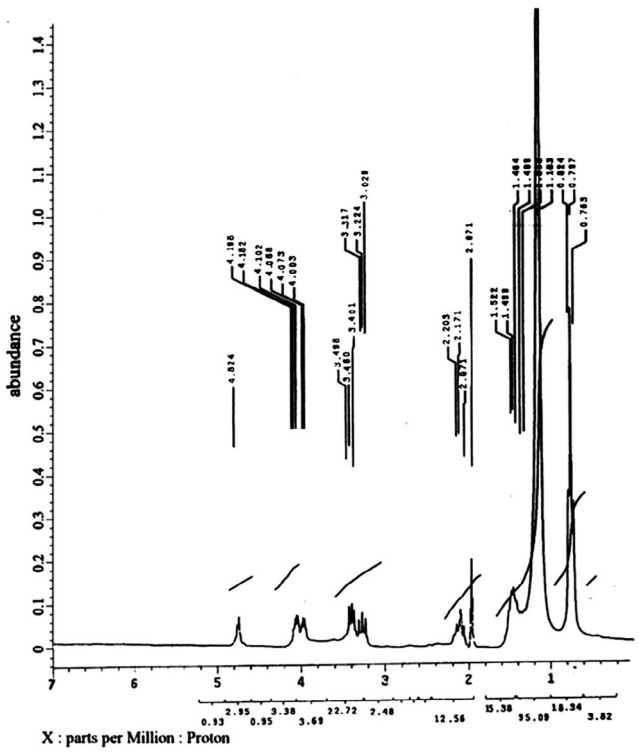

Fig 4 ^{1}H NMR spectra of surfactant II_C

of the synthesized surfactants I_b and II_b are shown in Figs 6 and 7) (similar figures for the other prepared inhibitors are provided in the supplementary materials) and the respective potentiodynamic parameters; corrosion potential E_{corr}, anodic and cathodic Tafel slope B_a and B_c corrosion current density i_{corr} and IE% are listed in Table 2.

It was cleared from the polarization profile the dramatic decrease of the cathodic current densities *via* the increase of the inhibitors concentrations which confirm that the inhibition of the cathodic process is official to the adsorption of the inhibitors on the aluminum surface, the parallel cathodic Tafel curves in Figs 6 and 7 also confirm that the mechanism of cathodic hydrogen evolution is not changed by the presence of the inhibitors (Asefi et al., 2009; Negm et al., 2010). Table 2 explains that both the anodic and cathodic slope were slightly altered by increasing the concentration of the investigated inhibitors, which confirm also that the mechanism of both aluminum dissolution and hydrogen evolution did not change and the inhibitors work without altering the mechanism but just by blocking the available surface area *i.e.* they only cause a part of the metal surface to be deactivated toward the corrosive medium (Fouda et al., 2014) it also confirms that these surfactants is a mixed type inhibitor. It is also shown in the table that the value of the corrosion potential E_{corr} does not change appreciably after the addition of surfactants which strengthens the same conclusions (Sayyah et al., 2014). It is cleared also from Table 2 that by increasing the concentration of the inhibitors the value of i_{corr} decreases and the IE% increase which suggests that at higher concentration of the inhibitor the protective layer tend to be more complete (Negm et al., 2014).

Furthermore, i_{corr} decrease and IE% increase as the no. of propylene oxide unites in the inhibitors increase and the values of IE% were in the following order $I_c > I_b > I_a$ also,

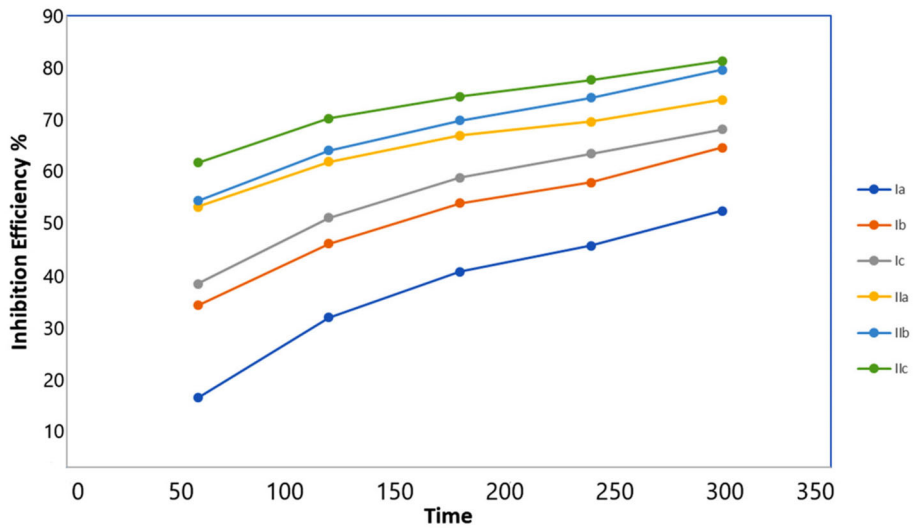

Fig 5 Effect of immersion time on inhibition efficiency in the presence of 5×10^{-5} Mol of inhibitors at 25 °C (data are mean of three replicates with relative error ~ 3.5%)

Table 1 Effect of inhibitors concentration on aluminum corrosion in 1.0 M HCl solution after 5 h (data are mean of three replicates with relative error ~ 3.5%)

Inhibitor	Inhibitors concentration (M) × 10^{-3}	Weight loss gm/cm^2	Inhibition efficiency %
	Free	0.1637	
I_a	0.01	0.0808	50.64
	0.05	0.080	51.13
	0.1	0.0714	56.38
	0.5	0.0641	60.84
	1.0	0.0424	74.09
I_b	0.01	0.0614	62.49
	0.05	0.0593	63.78
	0.1	0.0536	67.26
	0.5	0.0527	67.81
	1.0	0.0418	74.47
I_c	0.01	0.0611	62.68
	0.05	0.0534	67.38
	0.1	0.0518	68.36
	0.5	0.0417	74.53
	1.0	0.0347	78.80
II_a	0.01	0.0541	6.95
	0.05	0.0438	73.24
	0.1	0.0431	73.67
	0.5	0.0344	78.98
	1.0	0.0241	85.28
II_b	0.01	0.0413	74.77
	0.05	0.0341	79.23
	0.1	0.0262	83.99
	0.5	0.0221	86.49
	1.0	0.0211	87.11
IIc	0.01	0.0377	76.97
	0.05	0.0311	81.00
	0.1	0.0202	87.66
	0.5	0.0169	89.68
	1.0	0.0152	90.71

II c > II_b > II_a because as the no of propylene oxide unite increases the adsorption of the inhibitors on the surface of the metal increase causing more protection and covering of the surface of the metal. It is also clear from the table that the most effective inhibitor is II_c which has the higher IE% which can be correlated to the effect of the alkyl chain attached to the surfactant molecules as the alkyl chain length increases the IE% increase (Sakunthala et al., 2013; Shalby and Osman, 2002); therefore, the inhibition efficiency of $II_{a,\ b,\ c}$ > $I_{a,b,c}$.

By comparing IE% of the six samples under the same conditions, we can conclude that IE% were in the following order II_c > II_b > II_a > $I_{\ c}$ > $I_{\ b}$ > I_a (similar results were obtained by the weight loss method).

Electrochemical Impedance Spectroscopy

The impedance spectra (Nyquist plots) obtained for aluminum immersed in 1.0 M HCl free and inhibited using the synthesized surfactants with different concentrations I_b and II_b in comparison with the free acid solution at 298 k are shown in Figs 8 and 9 (similar figures for the other prepared inhibitors are provided in the supplementary materials), it was clear that as the surfactants doses increase, the diameter of the semicircle increases; indicating that the main controlling factor for aluminum corrosion is the charge transfer process, it was cleared also from the plots that by increasing the concentration of the inhibitors the resistance of the inhibitors solutions increased. From the impedance parameters given in Table 3, it was cleared that the value of the charge transfer resistance R_{ct} increases but the double layer capacitance C_{dl} value decreases upon adding the tested compounds, the increase of R_{ct} is as a result of replacing the water molecules continuously by the inhibitors molecules adsorbed on the metal surface (Fouda et al., 2019) which causes the corrosion rate to be decreased. Higher values of R_{ct} are associated normally with slower corroding system, while the decrease in C_{dl} is caused by either increasing the electric double layer thickness or by the decrease in the dielectric constant; confirming that the inhibitors act by adsorption in the metal/ solution interface (AL-abdali et al., 2019).The inhibition efficiencies calculated from Eq. (5) were followed the order $II_{\ c}$ > II_b > II_a > $I_{\ c}$ > $I_{\ b}$ >I_a which matches the results of both the polarization techniques and weight loss method.

Surface Activity and Thermodynamic Properties

The surface tension, critical micelle concentration (CMC), effectiveness (π_{CMC}), maximum surface excess (A_{max}), and minimum area (A_{min}) obtained from the prepared nonionic-anionic surfactants are shown in Table 4.

It has been shown that the surface tensions of the synthesized surfactants are lower than the surface tension of water; indicating that the surfactant molecules can be adsorbed at the liquid/ air interface.

The (CMC) is correlated to the concentration at which the surfactant monomers start aggregating to produce micelles; the CMC values were determined from Fig. 10 and listed in Table 4. It is clear from the table that by increasing the hydrophobicity of the molecules in series II the adsorption of the surfactant molecules at air-water interface decreases and thus the CMC values decrease (Tyagi and Tyagi, 2011). The lower values of the CMC indicate high repulsion between water and surfactant molecules in the aqueous phase which causes the adsorption of the inhibitors molecules to increase at the surface of the metal and increases the formation of the monolayer of the inhibitor on

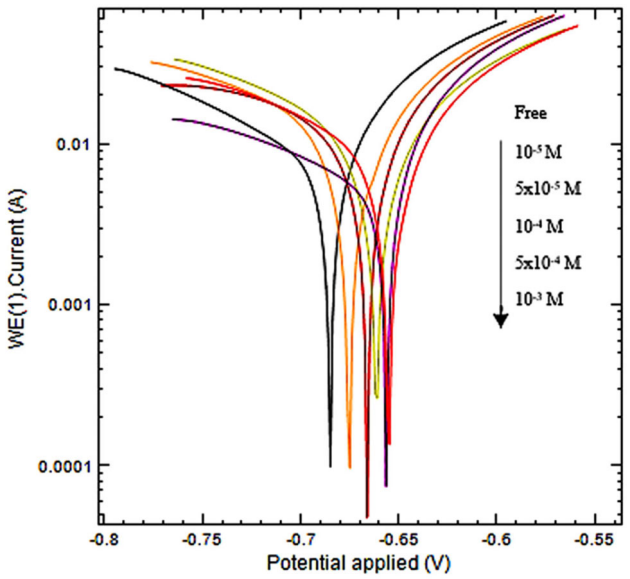

Fig 6 Potentiodynamic polarization curves for the corrosion of aluminum in 1 M HCl in the absence and presence of different concentration of I_b at scanning rate 2 mVS^{-1}

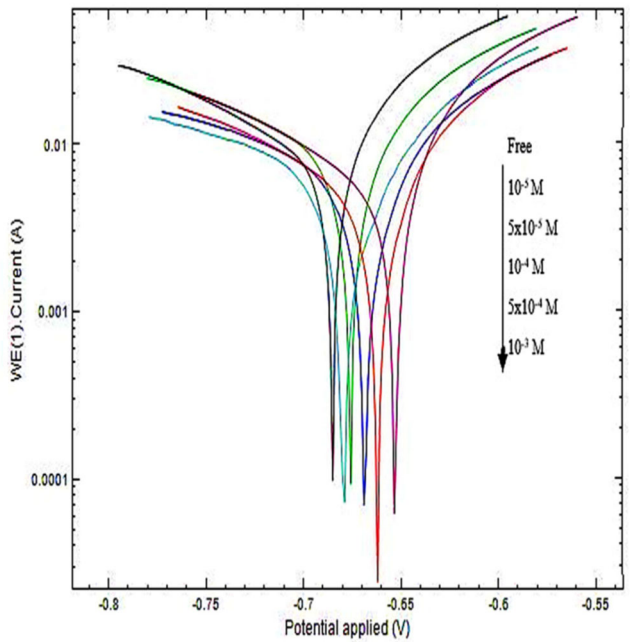

Fig 7 Potentiodynamic polarization curves for the corrosion of aluminum in 1 M HCl in absence and presence of different concentration of compound II_b at scanning rate 2 mVS^{-1}

the metal surface accordingly the inhibitor efficiencies increase.

Effectiveness π_{CMC} which is defined as the ability of the surfactant to reduce surface; therefore, surfactant with a higher π_{CMC} value has a higher affinity to be adsorbed at air-water interface than one with smaller π_{CMC} from the calculated values of π_{cmc} in Table 4; it was cleared that the sequence of the surfactant to be adsorbed at the interface are in the following order $II_c > II_b > II_a > I_c > I_b > 1_a$.

Gibb's adsorption equations are used to calculate the maximum surface excess concentration of the surfactant solutions Γ_{max} and the minimum area per molecule (A_{min}) (Rosen, 1981).

$$\Gamma_{max} = \frac{-1}{RT}\left(\frac{\delta\gamma}{\delta \ln C}\right)T \quad (7)$$

$$A_{min} = 10^{16}/\Gamma_{max}N \quad (8)$$

where $d\gamma/d\ln C$ is the slope of the plotted γ against log C in each case, R is the gas constant, T is the absolute temperature, C is the surfactant concentration, and N_A is Avogadro's number; it can be seen from Table 4 that as the propylene oxide units increased; the value of Γ_{max} decreased, while A_{min} increased. This is attributed to the increase of hydrophilicity of the surfactant molecules as propylene oxide units increase which increases the surfactant molecular size at the interface; causing the hydrophilic moiety of the surfactant and the metal surface to interact strongly (Rosen et al., 1983; Tadros, 2005). Moreover, increasing the hydrophobic chain length of the surfactants has led to increase in the value of Γ_{max}; as the alkyl chain length increased, the repulsion between the aqueous phase and the surfactants molecules increased; forcing the surfactant molecules to the interface. Furthermore, the increase in the value of A_{min} increases the efficiency of the inhibitors to protect the surface of the metal from the acidic medium. Finally, from the abovementioned data, it was found that the arrangement of the four values of CMC,π_{CMC},Γ_{max}, and A_{min} agrees with the sequences of IE% of the prepared inhibitors.

ΔG_{ad} and ΔG_{mic} are the standard free energy of adsorption and micellization, respectively, which measures the adsorption ability of the surfactants at the interface, or micellization in their solution was calculated using Eqs. (9) and (10) (Rosen, 1989) and shown also, in Table 4.

$$\Delta G_{mic} = 2.3RT\,(\log CMC) \quad (9)$$

$$\Delta Gads = \Delta Gmic - (0.6 \times \pi_{CMC} \times A_{min}) \quad (10)$$

where R is the universal gas constant, T is the absolute temperature (K). The negative values of ΔG_{mic} and ΔG_{ads} indicate that the adsorption and micellization of the surfactants molecules occurred spontaneously and the narrow difference between its values confirmed the equilibrium between the adsorbed molecules at the interface and the micellized molecules in the bulk. Furthermore, the higher negative values of ΔG_{ads} than those of micellization confirmed that the prepared surfactants have a higher tendency to be adsorbed at the air-water interface than micellize in the bulk of their solutions.

Table 2 Polarization parameters for aluminum corrosion in 1.0 M HCl solutions at different concentrations of the inhibitors

Inhibitors	Inhibitors conc (M) × 10^{-3}	B_a mV/dec	-B_c mV/dec	-E_{corr} mV	I_{corr} mA/cm^2	C.R mm/year	%I.E
	Free	54	117	667	6.7	79	—
I_a	0.01	34	35	661	3.4	31	49
	0.05	37	23	666	3.1	29	54
	0.1	40	21	656	2.7	24	60
	0.5	31	25	655	2.1	23	69
	1.0	19	29	670	1.9	23	72
I_b	0.01	45	95	668	2.7	40	60
	0.05	35	99	650	2.5	36	63
	0.1	43	92	658	2.2	31	67
	0.5	45	64	655	2.0	22	70
	1.0	42	59	652	1.7	21	74
I_c	0.01	53	32	670	3.1	28	55
	0.05	48	29	667	2.3	27	66
	0.1	75	16	660	2.1	24	69
	0.5	62	25	655	1.9	23	72
	1.0	50	23	650	1.6	18	76
II_a	0.01	56	37	676	2.7	36	60
	0.05	67	25	653	2.4	28	64
	0.1	57	34	668	2.1	22	69
	0.5	61	30	662	1.8	20	73
	1.0	47	34	679	1.4	15	79
II_b	0.01	50	30	680	2.4	41	64
	0.05	62	22	653	2.3	27	66
	0.1	54	25	649	1.9	25	72
	0.5	52	23	668	1.5	24	75
	1.0	29	35	679	1.2	14	83
II_c	0.01	77	32	661	2.2	34	67
	0.05	51	28	660	1.9	22	72
	0.1	47	27	659	1.8	21	73
	0.5	39	30	655	1.2	14	82
	1.0	38	31	661	1.0	12	85

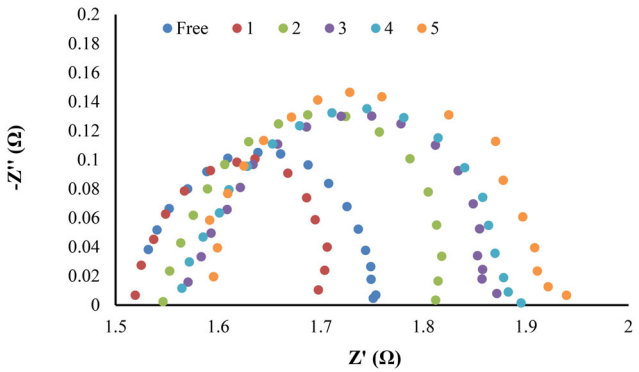

Fig 8 Nyquist plots of Al in 1 M HCl in the absence and presence of different concentrations of compound Ia (where 1 is 10^{-5} M, 2 is 5×10^5 M, 3 is 10^{-4} M, 4 is 5×10^{-4} M, and 5 is 10^{-3} M)

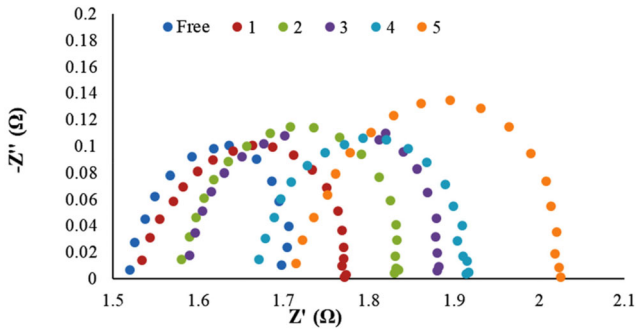

Fig 9 Nyquist plots of Al in 1 M HCl in the absence and presence of different concentrations of compound II_b (where 1 is 10^{-5} M, 2 is 5×10^5 M, 3 is 10^{-4} M, 4 is 5×10^{-4} M, and 5 is 10^{-3} M)

Table 3 Electrochemical parameters obtained from EIS measurements for aluminum corrosion in 1.0M HCl at different concentrations of the inhibitors

inhibitors	Inhibitor conc (M) $\times 10^{-3}$	Rs (Ohm cm^2)	R_{ct} (Ohm cm^2)	C_{dl} (F. cm^{-2})	IE%
Blank	Free	1.5	85	0.51	-
I_a	0.01	2.1	168	0.43	49.40
	0.05	1.7	185	0.33	54.04
	0.1	2.2	215	0.43	60.45
	0.5	1.9	287	0.22	70.30
	1.0	1.9	310	0.23	72.50
I_b	0.01	1.5	210	0.45	59.50
	0.05	1.6	235	0.41	63.82
	0.1	1.9	270	0.26	68.51
	0.5	1.8	287	0.23	70.38
	1.0	1.8	330	0.21	74.24
I	0.01	1.6	215	0.40	60.40
	0.05	1.9	256	0.29	66.80
	0.10	2.0	280	0.24	69.64
	0.50	2.3	310	0.22	72.58
	1.00	2.1	345	0.19	75.36
II_a	0.01	2.1	218	0.39	61.00
	0.05	1.6	240	0.33	64.50
	0.1	1.9	285	0.29	70.10
	0.5	1.8	320	0.27	73.43
	1.0	2.1	395	0.15	78.48
II_b	0.01	1.5	240	0.37	64.58
	0.05	1.6	255	0.29	66.66
	0.1	1.7	315	0.22	73.01
	0.5	2.1	346	0.20	75.43
	1.0	2.5	475	0.11	82.47
II_C	0.01	2.1	260	0.31	67.30
	0.05	2.0	309	0.21	72.40
	0.1	2.5	320	0.20	73.43
	0.5	2.3	470	0.14	81.90
	1.0	2.4	588	0.09	85.50

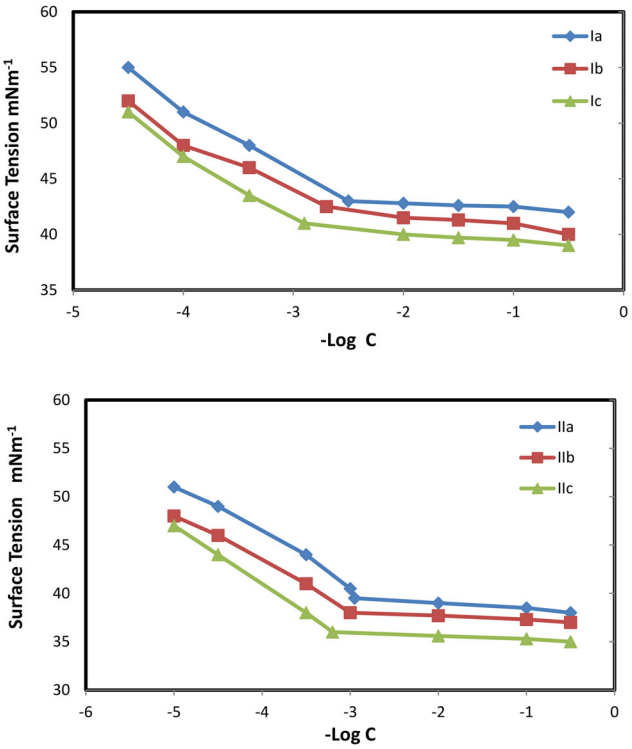

Fig 10 Surface tension vs log concentration of the prepared surfactants at 25 °C (Data are mean of three replicates with relative error ~ 3%)

Table 5 The biodegradation ratio of the synthesized nonionic-anionic surfactants in river water at 25 °C

Inhibitor	7 days degradation (%)	14 days degradation (%)	21 days degradation (%)	28 days degradation (%)
I_a	49	60	80	94
I_b	42	55	74	91
I_c	38	50	71	89
II_a	45	58	77	90
II_b	40	52	70	86
IIc	40	50	67	84

Table 4 Surface and thermodynamic parameters of the synthesized nonionic-anionic surfactants (data are mean of three replicates with relative error ~ 3%)

Inhibitor	Surface tension (mN m^{-1}) 0.1 wt% at 25°C	δ_{cmc} (mN m^{-1})	π cmc (mN m^{-1})	CMC Mol/L $\times 10^{-3}$	T_{max} (mol cm^{-2}) x 10^{-10}	A_{min} (nm^2)	$-\Delta G_{mic}$ KJ/mol	$-\Delta G_{ads}$ KJ/mol
I_a	42	43.0	29.0	3.162	9.41	1.764	14.246	14.276
I_b	40	42.5	29.5	1.992	8.79	1.888	15.385	15.419
I_c	39	41.0	31.0	1.584	8.35	1.988	15.956	15.993
IIa	38	39.5	32.5	1.525	7.22	2.299	16.050	16.095
II_b	37	38.0	34.0	0.100	6.95	2.389	22.793	22.842
II_c	35	36.7	35.3	0.063	6.28	2.644	23.936	23.992

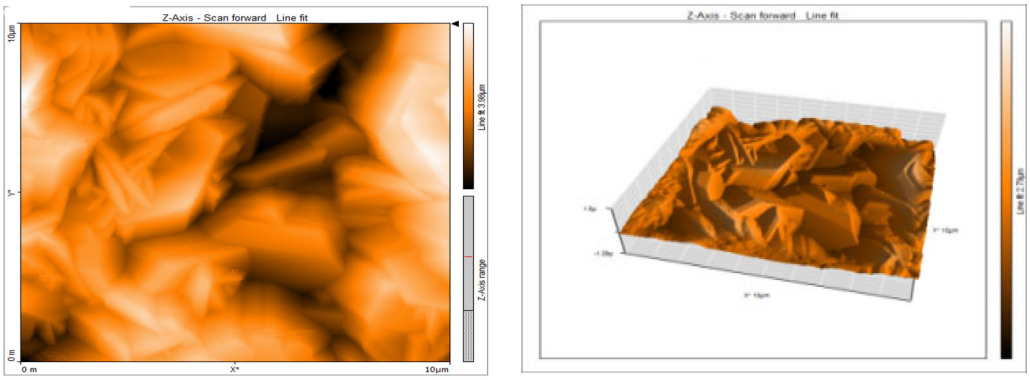

(a) Blank 2D and 3D respectively

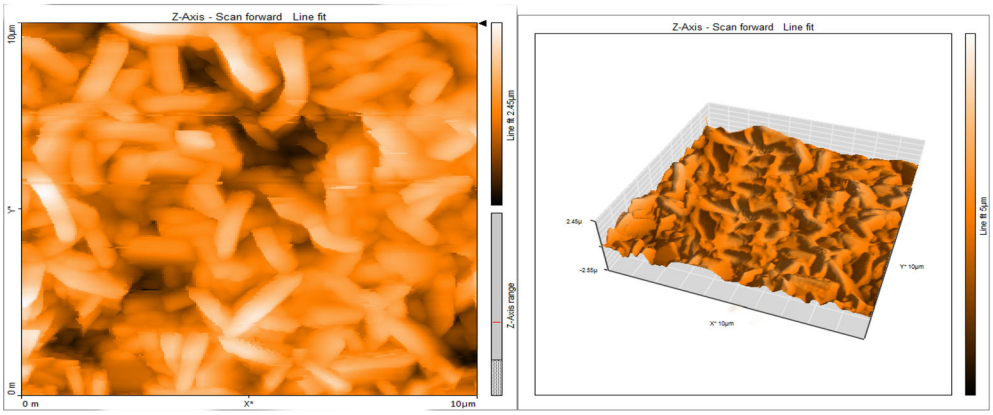

(b)Compound I_b 2D and 3D respectively

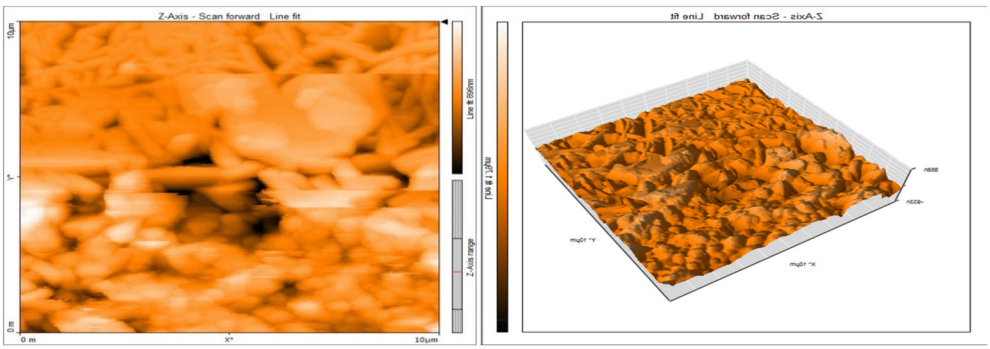

Compound II_b2D and 3D respectively(c)

Fig 11 2-D and 3-D atomic force images for aluminum surface after immersion in 1 M HCl (blank) (**a**) (**b**) inhibited with compound I_b (**c**) inhibited with compound II_b. (**a**) Blank 2D and 3D, respectively. (**b**) Compound I_b 2D and 3D, respectively. (**c**) Compound II_b2D and 3D, respectively

Table 6 AFM roughness data of inhibitors I_b and II_B

Inhibitor	Area, pm^2	S_a (nm)	Sp (nm)	Sv (nm)
Blank	100.8	671.30	2071.40	−209.90
I_b	100.8	190.97	1322.40	−868.45
II_b	100.8	110.31	528.49	−1044.90

Biodegradation

It was proved from the data in Table 5 that the biodegradation ratio of all the prepared compounds ranged from71 to 95% after 28 days of microorganisms' exposure. Moreover, the highest biodegradation ratio was attained for I_a and I_b at

94 and 91%, which has a small hydrophobic character and lower propylene oxide unit. It was found also from the table that there is a correlation between the biodegradation percent and the number of propylene oxide units in the inhibitors molecules. The biodegradation ratios match the international proposal of the biodegradable surfactants in drain water which is 70% after 28 days (Leal et al., 1994). Therefore, these surfactants can be categorized as biodegradable surfactants, the simplest pathway for the degradation for the prepared surfactants is a bacterial attack at either the hydrophobe or propylene oxide chain which results in shorting of its length (w-OE pathway) (Ratledge, 1994) and finally the hydrocarbon chain completely degraded.

Surface Examination

AFM is a very important technique which gives details about the surface morphology. The using of such technique is useful for corrosion research since it provides much information about the roughness of the examined surface (Motawe et al., 2019). Fig. 11 illustrated both the three- and two-dimensional images for the aluminum surface coupons after exposure to free acid and inhibited with surfactants, (the specimens of metal used to examine the surface morphology were used after immersion in 1 M HCl in the absence (blank) and presence of 10^{-3} M of the prepared inhibitors at 25 °C for 5 h) the figure shows that the roughness of the aluminum surface is highly reduced when using inhibitors as it forms adsorbing film that protects the metal surface from corrosive solution, the roughness decreases in the order of free $>I_b > II_b$.

Table 5 presents the roughness data of aluminum samples after exposure to solutions of 1.0 M HCl containing 10^{-3} M of each of the tested surfactants, for 1 day at 25°C. The table contains the roughness average (Sa), the peak height (Sp), and the valley depth (Sv). The data in Table 5 illustrated that all the measured values from the blank sample to the inhibited one follow the sequence; free $>I_b > II_b$. It is noticeable also that the aluminum surface becomes smoother upon adding the prepared surfactant as a result of adsorption of surfactants molecules on the metal surface. Furthermore, the effectiveness of the surfactants increases in the same order of inhibition efficiency attained from weight loss and electrochemical techniques (Table 6).

Conclusions

The prepared surfactants have inhibition efficiency for the aluminum corrosion in the acidic medium even at lower concentrations and the corrosion inhibition efficiency increases as the concentration, immersion time, and hydrophilic chain length increase. The results attained from electrochemical methods specified that the prepared compounds act as mixed-type inhibitors and the inhibition efficiencies attained from weight loss measurements, and electrochemical method were consistent with each other and followed the order $II_c > II_b > II_a > I_c > I_b > I_a$. The prepared compounds have good surface properties, and they tend to be adsorbed at the interface than micellization in the bulk of solution where both processes occur spontaneously as indicated by thermodynamic data. The biodegradability test indicted that these inhibitors are eco-friendly. AFM examination of the surface morphology illustrates that the roughness of the aluminum surface is highly reduced when using inhibitors and becomes smoother upon the addition of the prepared surfactant as a result of adsorption of surfactants molecules on the metal surface. Furthermore, the effectiveness of the surfactants increases in the same sequence of inhibition efficiency attained from weight loss and electrochemical techniques.

Conflict of Interest The authors declare that they have no conflict of interest.

References

Abdallah, M., Fouda, A. S., El Nagar, D. A. M., & Ghoneium, M. M. (2018a) Electrochemical and theoretical investigation for the protection of aluminum corrosion in hydrochloric acid using some azole derivatives. *Protection of Metals and Physical Chemistry of Surfaces*, **54**:1204–1212.

Abdallah, M., Gad, E. A. M., Al-Fahemi, J. H., & Sobhi, M. (2018b) Experimental and theoretical investigation by DFT on the some azole antifungal drugs as green corrosion inhibitors for aluminum in 1.0M HCl. *Protection of Metals and Physical Chemistry of Surfaces*, **54**:503–512.

Abdallah, M., Jahdaly, B. A. A. L., Sobhi, M., & Ali, A. I. (2015) Evaluation of some nonionic surfactants derived from hydroquinol compounds as corrosion inhibitors for carbon steel in hydrochloric acid. *International Journal of Electrochemical Science*, **10**: 4482–4494.

AL-abdali, F. H., Abdallah, M., & El-Sayed, R. (2019) Corrosion inhibition of aluminum using nonionic surfactant compounds with a six member heterocyclic ring in 0.1 M HCl solution. *International Journal of Electrochemical Science*, **14**:3509–3523.

Al-Khaldi, M. A., & Al-Qahtani, K. Y. (2013) Corrosion inhibition of steel by coriander extracts in hydrochloric acid solution. *Journal of Material and Environmental Science*, **4**:593–600.

Asefi, D., Arami, M., Sarabi, A. A., & Mahmoodi, N. M. (2009) The chain length influence of cationic surfactant and role of nonionic surfactants in controlling the corrosion rate of steel in acidic medium. *Corrosion Science*, **51**:1817–1821.

Azzam, E. M. S., & Abd El-Aal, A. A. (2013) Corrosion inhibition efficiency of the synthesized poly-12-(3-amino phenoxy) dodecane-1-thoil surfactant assembled on silver. *Egyptian Journal of Petroleum*, **22**:265–270.

Bardal, E. (2004) *Corrosion and protection (engineering materials and processes)*. London, England: Springer.

Bedair, M. A., El-Sabbahan, M. M. B., Fouda, A. S., & Elaryian, H. M. (2017) Synthesis, electrochemical and quantum chemical studies of some prepared surfactants based on azodye and Schiff base as corrosion inhibitors for steel in acid medium. *Corrosion Science*, **128**:54–72.

Chavda, S., Bahadur, P., & Aswal, V. K. (2011) Interaction between nonionic and gemini (cationic) surfactants: Effect of spacer chain length. *Journal of Surfactant and Detergent*, **14**:353–362.

Chen, W., Luo, H. Q., & Li, N. B. (2011) Inhibition effect of 2,5-dimercapto-1,3,4-thiadiazole on the corrosion of mild steel in sulphuric acid solution. *Corrosion Science*, **53**:3356–3365.

Fouda, A. S., Shalabi, K., & Mohamed, N. H. (2014) Corrosion inhibition of aluminum in hydrochloric acid solution using some chalcone derivatives. *International Journal of Innovative Research in Science Engineering and Technology*, **3**:319–329.

Fouda, A. S., Zahi, E. G., & Khalifa, M. M. A. (2019) Some new nonionic surfactants based on propane tricarboxylic acid as corrosion inhibitors for low carbon steel in hydrochloric acid solution. *Journal of Bio and Tribo-Corrosion*, **5**:31–42.

Granese, S. L., Rosales, B. M., Ovied, C., & Zerbino, J. O. (1992) The inhibition action of heterocyclic nitrogen organic compound on Fe and steel. *Corrosion Science*, **33**:1439–1453.

Hegazy, M. A., Ahmed, H. M., & El-Tabie, A. S. (2011) Investigation of the inhibitive effect of p-substituted 4-(N,N,N-dimethyl dodecylammonium bromide)benzylidene-benzene-2-yl-amine on corrosion of carbon steel pipelines. *Corrosion Science*, **53**:671–678.

Hellberg, P. (2003) Cleavable surfactants—Giving an unstable advantage. *Lipid Technology*, **15**:101–114.

John, M. G. C., & Haq, Z. (1977) Poly (mon n-alkyl itaconic acid esters) their preparation and some physical properties. *British Polymer Journal*, **9**:241–245.

Kaufman, J. G. (2000) *Introduction to aluminum alloys and tempers*. Novelty, OH: ASM International.

Leal, J. S., Gonzalez, J. J., Kaiser, K. L., Palabrica, V. S., Comelles, F., & Garcia, M. T. (1994) On the toxicity and biodegradation of cationic surfactant. *Acta Hydrochimica et Hydrobiologica*, **22**:13–21.

Lece, H. D., Kann, C. E., & Atakal, O. (2008) Difference in the inhibitive effect of some Schiff base compounds containing oxygen and sulfurdonors. *Corrosion Science*, **50**:1460–1468.

Li, X., Deng, S., & Fu, H. (2011) Inhibition by tetra decyl pyridinium bromide of the corrosion of aluminum in hydrochloric acid solution. *Corrosion Science*, **53**:1529–1539.

Li, X., Deng, S., & Xie, X. (2014) Experimental and theoretical study on corrosion inhibition of oxime compounds for aluminium in HCl solution. *Corrosion Science*, **81**:162–175.

Lif, A. H. (1998) Nonionic surfactants containing an amide group. *Surfactant Science Series*, **6**:177–200.

Liu, Z. Y., Li, Z. Q., Song, X. W., Zhang, J. C., Zhang, L., & Zhao, S. (2014) Dynamic interfacial tensions of binary nonionic-anionic surfactants mixtures at water- alkaline interface. *Fuel*, **135**: 91–98.

Mehdaoui, R., Khelifa, A., & Aaboubizian, A. (2015) Inhibiting effect of some synthesized surfactants from petroleum oil on the corrosion of aluminum in hydrochloric acid solution. *Research on Chemical Intermediates*, **41**:705–720.

Migahed, M. A., Zaki, E. G., & Shabban, M. M. (2016) Corrosion control in the tubing steel of oil wells during matrix acidizing operation. *RSC Advances*, **6**:71384–71396.

Motawe, M. M., El Hossiany, A., & Fouda, A. S. (2019) Corrosion control of copper in nitric acid solution using chenopodium extract. *International Journal of Electrochemical Science*, **14**:1372–1381.

Negm, N. A., Ahmed, F. M., EL Farargy, A. E., EL aboudy, A. H. S., & Ahmed, A. E. S. (2014) Novel biobased nonionic surfactants: Synthesis, surface activity and corrosion ihibition efficiency against aluminum alloy dissolution in acidic media. *Journal of Surfactants and Detergents*, **17**:1203–1214.

Negm, N. A., Ahmed, S. A., Abd-Elah, A. A., & Ashraf, T. (2016) Synthesis and surface activity of nonionic surfactants derived from Gallic acid. *Arab Journal Science*, **41**:67–73.

Negm, N. A., Al Sabagh, A. M., Migahed, M. A., Abdel Bary, H. M., & El Din, H. M. (2010) Effectiveness of some diquaterary ammonium surfactants as corrosion inhibitors for carbon steel in 0.5 MHCl solution. *Corrosion Science*, **52**:2122–2132.

Negm, N. A., Elkholy, Y. M., Ghuiba, F. M., Zahran, M. K., Mahmoud, S. A., & Tawfik, S. M. (2011) Benzothiazol-3-ium cationic schiff base surfactants: Synthesis, surface activity and antimicrobial applications against pathogenic and sulfur reducing bacteria in oil field. *Journal of Dispersion Science and Technology*, **32**: 512–518.

Negm, N. A., Tawfik, S. M., Bader, E. A., Abdou, M. I., & Ghuiba, F. M. (2015) Evaluation of some nonionic surfactants derived from vanillin as corrosion inhibitors for carbon steel during drilling processes. *Journal of Surfactants and Detergents*, **18**: 413–420.

Ratledge, C. (1994) *Biochemistry of microbial degradation* (p. 89). Amsterdam, The Netherlands: Kluwer.

Rosen, M. J. (1976) The relationship of structure to properties in surfactants IV. Effectiveness in surface or interfacial tension reduction. *Journal of Colloids and Interface Science*, **56**:320–328.

Rosen, M. J. (1981) Purification of surfactants for studies of their fundamental surface properties. *Journal of Colloid Interface Science*, **79**:587–598.

Rosen, M. J. (1989) *Surfactant and interfacial phenomena* (2nd ed., p. 151). New York, NY: Wiley.

Rosen, M. J., Dahanayake, M., & Cohen, A. (1983) Relationship of structure to properties in surfactants. 11. Surface and thermodynamic properties of N-dodecyl-pyridinium bromide and chloride. *Journal of Colloid and Surface A*, **5**:159–172.

Saban, S. M., El-Sukkary, M. M., Soliman, M. M., & El-Awady, M. Y. (2015) Inhibition of mild steel corrosion in acidic medium by vanillin cationic surfactants. *Journal of Molecular Liquids*, **203**:20–28.

Safek, S., Dura, B., Yurt, A., & Turkoglu, G. (2012) Shiff bases as corrosion for aluminum in HCl solution. *Corrosion Science*, **54**: 251–259.

Sakunthala, P., Vivekananthan, S. S., Gopiraman, M., Sulochana, N., & Vincent, A. R. (2013) Spectroscopic investigation of physicochemical interaction on mild steel in acidic medium by environmentally friendly green inhibitor. *Journal of Surfactants and Detergents*, **16**:251–263.

Sayyah, S. M., El Deeb, M. M., Abd El Rehim, S. S., Ghanem, R. A., & Mohamed, S. M. (2014) Experimental and theoretical evaluation on the effect of the terminal side chain of a polymeric surfactant on the inhibition efficiency of aluminum corrosion in acid medium. *Portugaliae Electrochimica Acta*, **32**:417–429.

Shalby, M. N., & Osman, M. M. (2002) Application of some commercial nonionic surfactant in the field of corrosion inhibition mater. *Corrosion*, **53**:827–836.

Singh, A. K., & Quraish, M. (2011) Investigation of the effect of disulfiran on corrosion of mild steel in hydrochloric acid. *Corrosion Science*, **53**:1288–1297.

Solmaz, R., Erman, M. M., & Kardas, G. (2008) Adsorption and corrosion inhibition effect of 1,1-thiocarbonyl diimidazole on mild steel in H_2SO_4 solution and synergistic effect of iodide ion. *Actaphysico-Chimica Sinica*, **24**:1185–1191.

Stjerndahl, M., & Holmberg, K. (2005) Synthesis, stability, and biodegradability studies of a surface active amide. *Journal of Surfactants and Detergents*, **8**:331–336.

Stjerndahl, M., Lundberg, D., & Holmberg, K. (2003a) Cleavable surfactants. *Surfactant Science Series*, **114**:317–460.

Stjerndahl, M., Van Ginkel, C. G., & Holmberg, K. (2003b) Hydrolysis and biodegradation studies of surface active esters. *Journal of Surfactants and Detergents*, **6**:319–324.

Tadros, T. F. (2005) *Applied surfactants: Principles and applications*. Weinheim: Wiley-VCH.

Tantawy, A. H., Asadov, Z. H., Azizov, A. H., Rahimov, R. A., & Zarbaliyeva, I. A. (2014) Synthesis of new, ecologically safe and efficient oil slick-collecting and dispersing agents based on oleic acid and its propoxylation products. *Arab Journal for Science & Engineering*, **39**:5437–5444.

Tawfik, S. M. (2015) Synthesis, surface, biological activity and mixed micellar phase properties of some biodegradable gemini cationic surfactants containing oxycarbonyl groups in the lipophilic part. *Journal of Industrial and Engineering Chemistry*, **28**:171–183.

Tewfik, S. A., & Negm, N. A. (2016) Vanillin-derived nonionic surfactants as green corrosion inhibitors for carbon steel in acidic environments. *Research on Chemical Intermediates*, **42**:3579–3584.

Tyagi, P., & Tyagi, R. (2011) Synthesis of bisphospho diester surfactants derived from tetradecanol and different methylene chains as a spacer derived from a, x-alkyl dibromides. *Tenside Surfactant Detergent*, **48**:293–300.

Wang, X. G., Yan, F., Li, Z. Q., Zhang, L., Zhao, S., An, J. Y., & Yu, Y. (2007) Synthesis and surface properties of several nonionic-anionic surfactants with straight chain alkyl-benzyl hydrophobic group. *Colloid and Surface A. Physicochemical & Engineering Aspects*, **302**:532–539.

Winston, R., & Uhlig, S. (2011) *Corrosion handbook* (3rd ed.). New York, NY: John Willey and Sons.

Xli, H., & Mu, G. (2005) Tween-40 as corrosion inhibitor for cold rolled steel in Sulphuric acid: Weight loss study, electrochemical characterization, and AFM. *Applied Surface Science*, **252**: 1254–1265.

Yuan-Ting, D., Hui-Long, W., Yao-Rung, C., Hui-Ping, Q., & Wen-Feng, J. (2017) Synthesisof baicalin derivatives as eco-friendly green corrosion inhibitors for aluminum in hydrochloric acid solution. *Journal of Environmental Chemical Engineering*, **5**: 5891–5901.

Zaho, G. X., & Zhu, B. Y. (2003) *Principles of surfactant action*. Beijing, China: China Light Industry Press.

Zapta-Loria, A. D., & Pech-Canul, M. A. (2014) Corrosion inhibition of aluminum in 0.1M HCl solution by glutamic acid. *Journal Chemical Engineering Communication*, **201**:855–869.

Zhang, Z., Gao, Z., Xu, F., & Zou, X. (2011) Adsorption and corrosion inhibitive properties of gemini surfactants in the series of hexanediyl-1,6-bis-(diethyl alkyl ammonium bromide) on aluminum in hydrochloric acid solution. *Colloide and Surfaces A: Physicochemical and Engineering Aspects*, **380**:191–200.